Title

Electronic cigarette aerosols induce oxidative stress-dependent cell death and NF-κB mediated acute lung inflammation in mice

Journal

Archives of Toxicology, 95(1)

ISSN

0340-5761

Authors

Ma, Tiancong

Wang, Xiang

Li, Liqiao

et al.

Publication Date

2021

DOI

10.1007/s00204-020-02920-1

Peer reviewed

HHS Public Access

Author manuscript

Arch Toxicol. Author manuscript; available in PMC 2022 January 01.

Published in final edited form as:

Arch Toxicol. 2021 January ; 95(1): 195–205. doi:10.1007/s00204-020-02920-1.

Electronic cigarette aerosols induce oxidative stress-dependent cell death and NF-κB mediated acute lung inflammation in mice

Tiancong Ma[1,2], **Xiang Wang**[1], **Liqiao Li**[2], **Bingbing Sun**[3], **Yifang Zhu**[2,*], **Tian Xia**[1,*]

[1]Division of Nanomedicine, Department of Medicine, David Geffen School of Medicine, University of California, Los Angeles, California 90095-1772, USA

[2]Department of Environmental Health Sciences, Jonathan and Karin Fielding School of Public Health, University of California, Los Angeles, California 90095-1772, USA

[3]State Key Laboratory of Fine Chemicals, School of Chemical Engineering, Dalian University of Technology, 2 Linggong Road, 116024, Dalian, China

Abstract

Electronic cigarette (e-cigarette) use has been linked to recent acute lung injury case clusters in over 2000 patients and dozens of deaths in the United States, however, the mechanism leading to lung injury is not certain although ultrafine particles, heavy metals, volatile organic compounds, and other harmful ingredients have been implicated. To systematically evaluate e-cigarette toxicity, we generated e-cigarette aerosols by varying the puff numbers (20 to 480), nicotine contents (0 to 24 mg/mL), and collected e-cigarette samples through an impinger system for biological assays. The calculated samples' concentration ranged from 1.96 to 47.06 mg/mL. THP-1 monocyte-differentiated macrophages, BEAS-2B bronchial epithelial cells, wild-type C57BL/6 mice, and NF-κB-luc transgenic mice were used to test the effects of these samples. E-cigarette samples showed cytotoxicity to THP-1 cells and BEAS-2B *in vitro*, leading to increased oxidative stress, inflammatory cytokine production with or without nicotine, and cell death. Furthermore, aerosol generated from PG is more toxic than VG. The toxicity of e-cigarette samples is at least partially due to the reactive oxygen species and aldehydes, which are generated during the aerosolization processes by the e-cigarette device. After NF-κB-luc mice exposed with e-cigarette samples by oropharyngeal aspiration, NF-κB expressions were observed in a dose-response fashion with or without nicotine. In addition, the e-cigarette samples induced neutrophil infiltrations, IL-1β

*Corresponding author Yifang@ucla.edu, txia@ucla.edu.

Authors' contributions: Conception and design of the work, the analysis and interpretation of data for the work, the drafting and revision of the manuscript, and approval of the final version to be published—TM, TX, and YZ; collection of data, the analysis and interpretation of data for the work, critical revision of key intellectual content, and approval of the final version to be published— TM, XW, LL, and BS.

Declarations

Conflicts of interest/Competing interests: The authors state that they have no conflicts of interest to declare

Availability of data and material (data transparency): Not applicable

Code availability (software application or custom code): Not applicable

production, oxidative stress marker heme oxygenase-1 expression in wild-type C57BL/6 mice. These results suggested that oxidative stress, pro-inflammatory, NF-κB pathway activation, and cell death are involved in e-cigarette aerosols induced acute lung inflammation.

Keywords

Electronic cigarette aerosol; acute lung inflammation; oxidative stress; NF-κB pathway; aldehyde

Introduction

Electronic cigarette (e-cigarette) is marketed as a smoking cessation device for traditional tobacco cigarettes (t-cigarette). According to Adroit Market Research (2018), the global e-cigarette market value is expected to grow over $48.9 billion by 2025, with the largest revenue in the United States (Adroit Market Research 2018). It is generally agreed that compared with t-cigarette, e-cigarette aerosols contain lower levels of toxic chemicals. Thus, it should be a safer alternative to t-cigarette (McAuley et al. 2012; Romagna et al. 2013). However, the lung toxicity of e-cigarette has raised much attention (Bolt 2020). Recently, a multistate outbreak of e-cigarette or vaping product use–associated lung injury (EVALI) has resulted in over 2000 patients and dozens of deaths in the United States (Davidson et al. 2019; Krishnasamy 2020). The majority of the patients presented with acute respiratory symptoms and bilateral lung infiltrates on chest imaging (Henry et al. 2019). Though tetrahydrocannabinol (THC) and vitamin E acetate had been found strongly related to the EVALI, there is still limited knowledge regarding the acute lung inflammation of e-cigarette aerosols and the mechanism of toxicity (Blount et al. 2019; Feldman et al. 2020; Krishnasamy 2020).

One significant difficulty lies in the considerable variations in device design and diverse e-liquid compositions, including propylene glycol (PG) and/or vegetable glycerin (VG) that are spiked with nicotine, flavorings, and other additives. It is estimated that nearly 500 brands of e-cigarette with 7,700 flavors will be in the United States marketplaces before the Food and Drug Administration (FDA) can fully evaluate them (American Lung Association 2016). Another difficulty is the complexity of aerosols containing both chemicals and particulates. Several studies, including ours, have found significant amounts of fine ($PM_{2.5}$) and ultrafine particles (UFPs) in e-cigarette aerosols (Fuoco et al. 2014; Zhao et al. 2016). A recent review has summarized that the concentration of PG and VG was most abundant (i.e., greater than 1500 μg/puff) compared to other chemicals in e-cigarette aerosols (Li et al. 2020). In addition, the nicotine level in e-cigarette aerosols was found comparable to that in t-cigarette aerosols (Li et al. 2020). Toxic and carcinogenic compounds, like carbonyl compounds (Farsalinos et al. 2015; Kosmider et al. 2014), and toxic metals including Ni, Cu, and Fe have also been reported (Lerner et al. 2015; Saffari et al. 2014) in e-cigarette aerosols. This is in agreement with our previous results collected in normal human oral keratinocytes (NHOKs), showing e-cigarette aerosols are capable of inducing oxidative stress and unfolded protein response, which subsequently leads to cytotoxicity (Ji et al. 2019; Ji 2016). Although informative, these findings are obtained from specific device and e-liquid formulation that do not cover the wide range of e-cigarettes on the market. Thus, a

systematic approach is needed to elucidate the link between e-cigarette device features and key e-liquid components and their toxic potential.

In this study, we generated e-cigarette aerosols by varying the puff numbers, nicotine contents, and e-liquid compositions, which were collected through an impinger system. The collected e-cigarette aerosol samples in terms of particle size, shape, hydrodynamic size, charge, and metal contents were characterized. Their cytotoxic and pro-inflammatory effects on THP-1 monocyte-differentiated macrophages and BEAS-2B epithelial cells *in vitro* and acute lung inflammation using NF-κB-luc transgenic mice were tested. In addition, aldehydes, formaldehyde, and reactive oxygen species (ROS) concentration in e-cigarette samples were measured to reveal the potential mechanism of lung toxicity.

Methods

Experimental details on the characteristic of e-cigarette samples, cell culture, 3-(4,5-dimethylthiazol-2-yl)-5-(3-carboxymethoxyphenyl)-2-(4-sulfophenyl)-2H-tetrazolium (MTS) assay, adenosine triphosphate (ATP) assay, glutathione (GSH) content, aldehyde, and formaldehyde content, ROS generation measurement, animal model construction and *in vivo* imaging, Western Blotting, together with the collecting efficiency and the mass distribution in aerosols samples, are provided in Supplemental Materials.

Acquisition of E-cigarette Samples.

A tank-style e-cigarette device (i.e., Vapor-fi model Volt Hybrid Tank) equipped with a refillable tank, high capacity batteries, and adjustable power settings was used in this study. To avoid unknown compounds in the commercial e-liquids (Flora et al. 2016), we prepared homemade flavorless e-liquids from individual chemical compounds of PG ($C_3H_8O_2$, ≥ 99.5%), VG ($C_3H_8O_3$, ≥ 99.5%), and nicotine ($C_{10}H_{14}N_2$, ≥ 99%). A 30/70 mixture of PG/VG along with nicotine levels ranging from 0.0% to 2.4% (0 to 24 mg/mL) in the e-liquid was investigated in this study. Pure PG and VG were also used individually to compare their toxic effects.

E-cigarette aerosols were generated using an in-house made puffing machine composed of a compressed air source and a programmable timer to power the e-cigarette device at 3.0 V. The HEPA filtered air was continuously pushed through the e-cigarette tank at an airflow rate of 1 L/min. The e-cigarette device was controlled to repeat a continuous puffing cycle (i.e., 4 s puff duration, every 30 s) to mimic a typical puff topography of e-cigarette users (Behar et al. 2015; Farsalinos et al. 2013; Hua et al. 2013; Misra et al. 2002). Following the puffing protocol, we studied three exposure conditions: 20, 120, and 480 puffs.

The e-cigarette aerosols were collected by a water or cell culture media (20 mL) filled impinger (BioSampler, SKC Inc, Eighty-Four, PA) to obtain e-cigarette samples.

Statistical Analysis

Mean and standard deviation (SD) were calculated for each parameter. Results were expressed as mean ± SD of multiple determinations. Comparisons of each group were

evaluated by one-way ANOVA and pairwise t-test with Bonferroni. A statistically significant difference was assumed when p was <0.05.

Results

Physicochemical Characterization of E-cigarette Nanoparticles in the Liquid Phase

E-cigarette aerosols with different nicotine levels (0, 1.2 %, 2.4 %) were collected by a water or cell culture media filled impinger. This method has a high efficiency (80%, 1.96 mg/puff) in collecting aerosols into suspension to enable accurate dose control. The particle size distribution of the collected aerosols was calculated and showed in Figure S1. Most of these particles (95.9%) were smaller than 2.5 μm. E-cigarette aerosol particles in suspension were characterized by using TEM, which indicated that the particles in the e-cigarette aerosols were in irregular shapes (Figure 1). The Dynamic Light Scattering (DLS) measurement showed that the aerosols with nicotine had a smaller hydrodynamic size than samples without nicotine in water, ranging from 129.3 to 454.0 nm (Table 1). All the particles showed negative zeta-potentials in water ranging from −9.3 to −39.8 mV (Table 1). Zeta-potential results indicated that aerosols without nicotine were not stable in water and were easier to form larger aggregates. This was verified by the TEM and DLS results. The metal and metalloid components of each sample were also determined by ICP-MS (Table 2). A total of 18 metal and metalloid elements were analyzed, where sodium (Na), phosphorus (P), Calcium (Ca) were the most abundant elements. Due to the diluted concentration of these elements, their toxic effects could be excluded based on our previous studies (Li et al. 2008; Nemery 1990; Xia et al. 2011).

E-cigarette Aerosol Induced Cytotoxicity and Oxidative Stress *in vitro*.

The cytotoxicity profiles for collected e-cigarette samples in THP-1 cells, a human monomyelocytic leukemia cell line, were determined by using MTS and ATP assays. THP-1 macrophages were treated with e-cigarette samples with different nicotine levels for 24 h. The results show that the number of puffs and % of nicotine-dependent increased in cell toxicity induced by e-cigarette aerosols (Figures 2a and 2b). The aerosols collected at higher number puffs (480 puffs) induced more potent cytotoxicity in THP-1 cells than those collected at lower number puffs (20 puffs). At the same puff numbers, especially 480 puffs, the higher nicotine percent samples showed higher toxicity. Based on our previous studies, it was demonstrated that oxidative stress plays a major role in particle-induced cytotoxicity (Li et al. 2008). Thus, GSH depletion assay was performed. It was demonstrated that samples with the highest nicotine level and highest number of puffs induced an obvious decrease in GSH levels in cells (Figure 2c). In addition to the cytotoxicity and oxidative stress, e-cigarette aerosols could also induce a pro-inflammatory effect, as demonstrated by the production of IL-1β and TNF-α in THP-1 cells. Figure 2d showed the number of puffs and % of nicotine-dependent IL-1β production. The highest number of puffs (480 puffs) can affect IL-1β significantly. The e-cigarette aerosol samples without nicotine (0%) induced more cytokine production than those with higher nicotine levels (1.2% and 2.4%). Samples collected at 0% and 1.2% nicotine level with 480 puffs induced similar cell viability and significantly different cytokine productions. As shown in Figure 2e, higher nicotine levels decreased the TNF-α production. In summary, aerosols can affect pro-inflammatory factors

at a higher number of puffs (480 puffs, for example), and nicotine may inhibit the production of IL-1β and TNF-α in THP-1 cells.

BEAS-2B was also used to determine the toxicity profiles of e-cigarette aerosols. After 24-h exposure to different e-cigarette aerosols, BEAS-2B cells showed similar trends and a higher resistance comparing the THP-1 cells. In the MTS assay (Figure 3a), only the highest puff number has significant toxicity, and a higher nicotine level with 480 puffs induced lower cell viability. As shown in Figures 3b and 3c, no significant toxicity for BEAS-2B cells was observed besides the 2.4% nicotine concentration at 480 puffs sample in the ATP assay and the GSH determination. The expression of IL-8 and TGF-β1 by e-cigarette aerosols treated BEAS-2B cells were measured with ELISA. It was found that e-cigarette aerosols at 20 puffs induced a significant increase in TGF-β1 production, while higher puff numbers did not. The 480 puffs reduced the production of IL-8 (Figure 3e). The expression of IL-8 decreases at a higher nicotine level, suggesting that nicotine may inhibit IL-8 production. The nicotine influence on the expression of TGF-β1 was not observed.

The toxicity of commercial e-liquid with different nicotine levels (0%, 1.2%, 2.4%) was also examined in THP-1 cells (Figures S2a and S2b). As shown in Figure S2c, intracellular GSH levels suggested that commercial e-liquids induced oxidative stress-dependent cell death. At the same nicotine level, commercial e-cigarette samples showed more toxic as the puff number increased. The HO-1 expression in cell extracts increased at the higher puff number (Figure S2e). For 120 puff samples, the e-cigarette aerosol induced less acute cytotoxicity as nicotine was increased. As shown in Figure S2f, the nicotine influence on the expression of IL-1β was not observed.

The Role of Individual E-liquid Component in Inducing Cytotoxicity and Oxidative Stress *in vitro*.

To explore mechanisms of the e-cigarette aerosol-induced cytotoxicity and pro-inflammatory effects, the component in e-liquid (PG, VG, and nicotine) were investigated *in vitro*. We used pure PG and pure VG as the e-liquid to prepare samples. As shown in Figures 4a and 4b, comparing with VG, PG shows much more toxicity to THP-1 cells. GSH results indicated this injury might be induced by oxidative stress (Figure 4c). Neither PG nor VG can promote IL-1β production (Figure 4d). In addition, pure PG and VG without going through the heating process in the e-cigarette device were added into the cell culture medium directly, and the toxicity of these samples was tested. The results (Figure S3) suggested that PG and VG exhibit no significant cytotoxicity to the THP-1 cells when the concentration is below 40 mg/mL, which is similar to 480 puffs. This indicates that the heating process plays a critical role in causing the cytotoxicity. It is worth noting that PG showed more toxicity for THP-1 cells, even without the combustion process at 100 mg/mL.

We also determined the cytotoxicity of nicotine by directly adding it into the cell culture media at different concentrations. For THP-1 cells, the toxicity of nicotine does not strictly depend on its concentration (Figures S4a and S4b). As shown in Figure S4c, the GSH measurements have similar trends. Higher nicotine concentrations can inhibit the expression of IL-1β comparing with lower nicotine concentrations (Figure S4d).

E-cigarette Induced ROS and Generation of Aldehyde.

As we demonstrated above, e-cigarette aerosols could generate cellular oxidative stress. One possibility is that e-cigarette aerosols could induce abiotic ROS. Thus, the ROS concentration induced by e-cigarette samples in water was measured by DCF assay. As shown in Figure 5a, e-cigarette samples significantly enhanced DCF fluorescence, suggesting increased total abiotic ROS generation. The DCF fluorescence intensity at 525 nm was shown in Figure 5b. However, despite the increasing trend of ROS generation in terms of puff numbers and nicotine content, there is no statistical difference among all the samples.

In order to explore mechanisms of the e-cigarette aerosol induced cytotoxicity and pro-inflammatory effects, we measured the total aldehyde and formaldehyde content in the samples. The e-cigarette aerosols with a PG/VG ratio of 30/70 at two nicotine levels (0%, 2.4%) in cell culture media and water at low (120 puffs) and high (480 puffs) doses were tested (Figures 5c and 5d). The results showed that all the samples contained aldehyde, ranging from 2.45 to 28.92 μM, while samples of high puffs had a higher aldehyde level than that of low puffs (Figure 5c). A similar trend was also observed in the measurement of formaldehyde content in these samples (Figure 5d). Cytotoxicity assessments confirmed that aldehyde and formaldehyde could trigger a significant decrease in cell viability (up to 70 %) within the dose range measured in the e-cigarette samples (Figures 5e and 5f). These data showed that the aldehyde, especially the formaldehyde content in the e-cigarette aerosols, plays an important role in the cytotoxicity and pro-inflammatory effects.

E-cigarette Induced Acute Lung Inflammation by Activation of the NF-κB Pathway.

To verify if the *in vitro* toxicity could be replicated *in vivo*, an animal study using transgenic NF-κB-luc (inflammation, stress responses) mice from Jackson laboratory was performed to visually observe the responses of e-cigarette aerosols with and without nicotine in the lung. After lung exposure of e-cigarette aerosols for 24 h, the images of the lung were taken *ex vivo* after luciferin injection by *in vivo* imaging system (IVIS) (Nel et al. 2013). As seen in Figure 6a, the NF-κB-luc mice were used to show the activation of the NF-κB pathway in the lungs of animals receiving ZnO NPs (positive control, 2 mg/kg) and e-cigarette aerosols with different nicotine levels (0% and 2.4%). The data clearly showed that e-cigarette aerosols could activate the inflammatory pathway and induce stress responses (Figure 6b). Moreover, a 24-h *in vivo* study using wild-type C57BL/6 mice was conducted to confirm the inflammatory effect of e-cigarette aerosols in the lung. ZnO NPs at 2 mg/kg was used as a positive control. The results showed clear dose-dependent acute inflammatory effects in mice with high puff e-cigarette aerosols inducing more IL-1β production (Figure 6c) and neutrophil infiltration (Figures 6d and 6e) in BALF than lower number puff e-cigarette aerosols. The tissue HO-1 expression was also increased in the lung in a puff-dependent manner post-exposed to e-cigarette aerosols (Figure 6f). This effect was also confirmed by different levels of focal inflammation in the lung, as demonstrated by hematoxylin and eosin (H&E) staining (Figure 6g). These results showed that e-cigarette aerosols could induce acute lung inflammation and the mechanism also involves oxidative stress and NF-κB pathway.

Discussion

Major e-liquid components PG and VG are widely used in medicines, cosmetics, or food products. However, it is difficult to identify the safety of these two chemicals as e-liquids. There are many decomposition pathways of PG and VG in the process of e-cigarette aerosol generation, suggesting that they may induce toxicity by the byproducts (Strongin 2019). In our study, comparing with VG, PG has much more toxicity after e-cigarette aerosol generation to THP-1 cells. We detected a considerable amount of aldehyde generation by e-cigarette aerosols in our study (Fig. 5), which could induce oxidative stress and cell death (Li et al. 2020; O'Brien et al. 2005).

Nicotine is generally recognized as the major reason why people consume tobacco. The contrasting effects of nicotine in the cytotoxicity of THP-1 cells and BEAS-2B cells were observed. In addition, as shown in Figure 2d and Figure S4d, nicotine decreases the expression of IL-1β, which is one of the major pro-inflammatory effects (Ulloa 2005; Wang et al. 2003). This indicates that under certain conditions, nicotine might trigger adaptive/protective response, a theory that agrees with some reports in the literature (Guan et al. 2003; Hedstrom et al. 2013).

ROS are toxic to cells at higher levels due to the oxidative stress they exert by their reaction with proteins, lipids, and nucleic acids as well as cellular organelles, including mitochondria (Mates 2000; Xia et al. 2006). The appropriate cellular response to ROS production is critical to prevent further oxidative damage and to maintain cell survival. Among the oxidative stress-responsive signaling pathways, NF-κB is one of the most important pathways, and it is composed of five related transcription factors: p50, p52, RelA (p65), c-Rel and RelB (Reuter et al. 2010; Valko et al. 2006). It is responsible for controlling ROS levels *via* increased expression of antioxidant proteins such as SOD. As the level of oxidative stress increases, NF-κB induces the expression of various pro-inflammatory genes, including those encoding cytokines and chemokines, and also participates in inflammasome regulation. In addition to mediating the induction of various pro-inflammatory genes in innate immune cells, NF-κB also has a role in regulating the activation of NLRP3 inflammasomes that controls IL-1β production by expression of NLRP3 and pro-IL-1β proteins (Zhong et al. 2016). ROS could activate NF-κB by inducing IKK activation and IκBα phosphorylation, which result in the degradation of IκBα. NF-κB then translocates to the nucleus to activate target genes. In addition, the phosphorylation of RelA that is influenced by ROS-dependent processes leads to greater NF-κB activation. In NF-κB-luc mice, we observed enhanced NF-κB activation in the lung but no other organs in a dose-response fashion. However, there are no obvious differences in the presence or absence of nicotine.

Compared to e-cigarette, the t-cigarette generates thousands of chemicals in the burning process, including carbon monoxide, acrolein, nicotine, acetaldehyde, ammonia, polycyclic aromatic hydrocarbons, N-nitrosamines, misc organic compounds, and so on (Flouris et al. 2013; Lee et al. 2012). In e-cigarette aerosols, besides PG, VG, and nicotine, we also found aldehyde, especially formaldehyde. According to the literature, acetaldehyde, propanal, acetone, benzene, nickel, cadmium chromium were also identified in e-cigarette aerosols.

However, most chemicals were found at lower levels compared to those in t-cigarette smoke (Li et al. 2020). The results in this study suggested that t-cigarette and e-cigarette induced similar pro-inflammatory effects, such as NF-κB activation and TNF-α production, which was reasonable due to the similarity in some important toxic chemical components. However, many chemicals generated from t-cigarette have carcinogenic effects, and the complete chemical compositions of e-cigarette aerosols and their molecular and cellular effects on carcinogenesis have not been determined. Future studies are needed to determine the chemical compositions in e-cigarette aerosols and their cellular effects, including mutagenesis.

In addition to customized e-liquids, commercial e-liquids with the same nicotine level (0%, 1.2%, and 2.4%) was used to generate aerosol samples, and the results were shown in supplemental materials (Figure S2). Compared with our homemade e-liquids, which only consist of PG, VG, and nicotine, commercial e-liquids showed significant cytotoxicity to THP-1 cells at 120 puffs. These results indicated that commercial e-liquids might contain unknown compositions beyond PG/VG, which contribute to cytotoxicity. Thus, a detailed and precise label for ingredients of e-liquids is necessary for us to understand and evaluate their health effect.

Conclusions

Samples were prepared by collecting e-cigarette aerosols generated from different e-liquids, which consist of PG, VG, and nicotine. By variation of the puff number and nicotine content, the toxicity of the e-cigarette samples was systematically investigated *in vitro* and *in vivo*. E-cigarette samples generated ROS, induced oxidative stress, pro-inflammatory cytokine production, and cytotoxicity in THP-1 cells and BEAS-2B cells. In addition, e-cigarette samples induced oxidative stress and NF-κB expression in the animal lung after exposure by oropharyngeal aspiration. They also induced acute lung inflammation, including neutrophil infiltration, IL-1β production, and expression of an oxidative stress marker, heme oxygenase-1. PG and VG induced cytotoxicity depends on the puff number, and PG induced higher cytotoxicity than VG. Independent and concentration-dependent cytotoxicity for nicotine was observed, and nicotine's protective effects were also noticed. The toxicity of e-cigarette samples was at least partially due to the generation of abiotic ROS and aldehydes, which were generated during the aerosolization processes by the e-cigarette device. These results suggested that oxidative stress, pro-inflammatory pathway activation (e.g., NF-κB, NLRP3 inflammasome), and cell death were involved in e-cigarette induced acute lung inflammation, which provided valuable information to understand the cause of EVALI.

Supplementary Material

Refer to Web version on PubMed Central for supplementary material.

Acknowledgments

Funding: This study received support from the National Heart Lung and Blood Institute (Grant number: NHLBI R01 HL139379) (Y.Z).

Reference.

Adroit Market Research (2018) Global E-Cigarette Market Size 2017 by Type (Disposable, Rechargeable, Modular), By Region and Forecast 2018 to 2025.

American Lung Association (2016) E-cigarettes and Lung Health. American Lung Association. http://www.lung.org/stop-smoking/smoking-facts/e-cigarettes-and-lung-health.html. Accessed Augest 30 2017

Behar RZ, Hua M, Talbot P (2015) Puffing Topography and Nicotine Intake of Electronic Cigarette Users PloS One 10:e0117222 doi:10.1371/journal.pone.0117222

Blount BC et al. (2019) Vitamin E Acetate in Bronchoalveolar-Lavage Fluid Associated with EVALI New England Journal of Medicine 382:697–705 doi:10.1056/NEJMoa1916433

Bolt HM (2020) Electronic cigarettes and vaping: toxicological awareness is increasing Archives of Toxicology 94:1783–1785 doi:10.1007/s00204-020-02786-3 [PubMed: 32440856]

Davidson K et al. (2019) Outbreak of Electronic-Cigarette-Associated Acute Lipoid Pneumonia - North Carolina, July-August 2019 MMWR Morb Mortal Wkly Rep 68:784–786 doi:10.15585/mmwr.mm6836e1 [PubMed: 31513559]

Farsalinos KE, Romagna G, Tsiapras D, Kyrzopoulos S, Voudris V (2013) Evaluation of Electronic Cigarette Use (Vaping) Topography and Estimation of Liquid Consumption: Implications for Research Protocol Standards Definition and for Public Health Authorities' Regulation Int J Environ Res Public Health 10:2500–2514 doi:10.3390/ijerph10062500

Farsalinos KE, Voudris V, Poulas K (2015) E-cigarettes generate high levels of aldehydes only in "dry puff' conditions Addiction 110:1352–1356 doi:10.1111/add.12942 [PubMed: 25996087]

Feldman R, Meiman J, Stanton M, Gummin DD (2020) Culprit or correlate? An application of the Bradford Hill criteria to Vitamin E acetate Archives of Toxicology 94:2249–2254 doi:10.1007/s00204-020-02770-x [PubMed: 32451600]

Flora JW et al. (2016) Characterization of potential impurities and degradation products in electronic cigarette formulations and aerosols Regulatory Toxicology and Pharmacology 74:1–11 doi:10.1016/j.yrtph.2015.11.009 [PubMed: 26617410]

Flouris AD et al. (2013) Acute impact of active and passive electronic cigarette smoking on serum cotinine and lung function Inhal Toxicol 25:91–101 doi:10.3109/08958378.2012.758197

Fuoco FC, Buonanno G, Stabile L, Vigo P (2014) Influential parameters on particle concentration and size distribution in the mainstream of e-cigarettes Environmental Pollution 184:523–529 doi:10.1016/j.envpol.2013.10.010 [PubMed: 24172659]

Guan ZZ, Yu WF, Nordberg A (2003) Dual effects of nicotine on oxidative stress and neuroprotection in PC12 cells Neurochem Int 43:243–249 doi:10.1016/S0197-0186(03)00009-3 [PubMed: 12689604]

Hedstrom AK, Hillert J, Olsson T, Alfredsson L (2013) Nicotine might have a protective effect in the etiology of multiple sclerosis Mult Scler 19:1009–1013 doi:10.1177/1352458512471879 [PubMed: 23319071]

Henry TS, Kanne JP, Kligerman SJ (2019) Imaging of Vaping-Associated Lung Disease N Engl J Med 381:1486–1487 doi:10.1056/NEJMc1911995

Hua M, Yip H, Talbot P (2013) Mining data on usage of electronic nicotine delivery systems (ENDS) from YouTube videos Tobacco Control 22:103–106 doi:10.1136/tobaccocontrol-2011-050226 [PubMed: 22116832]

Ji EH et al. (2019) E-cigarette aerosols induce unfolded protein response in normal human oral keratinocytes J Cancer 10:6915–6924 doi:10.7150/jca.31319 [PubMed: 31839827]

Ji GSB; Zhao T; Shu S; Chang CH; Xia T; Zhu Y; Hu S (2016) Characterization of electronic cigarette aerosol and its induction of oxidative stress response in oral keratinocytes PLoS One 11:e0154447 doi:10.1371/journal.pone.0154447

Kosmider L, Sobczak A, Fik M, Knysak J, Zaciera M, Kurek J, Goniewicz ML (2014) Carbonyl Compounds in Electronic Cigarette Vapors: Effects of Nicotine Solvent and Battery Output Voltage Nicotine & Tobacco Research 16:1319–1326 doi:10.1093/ntr/ntu078 [PubMed: 24832759]

Krishnasamy VP (2020) Update: Characteristics of a Nationwide Outbreak of E-cigarette, or Vaping, Product Use–Associated Lung Injury—United States, August 2019–January 2020 vol 69.

Lee J, Taneja V, Vassallo R (2012) Cigarette Smoking and Inflammation: Cellular and Molecular Mechanisms Journal of Dental Research 91:142–149 doi:10.1177/0022034511421200 [PubMed: 21876032]

Lerner CA et al. (2015) Environmental health hazards of e-cigarettes and their components: Oxidants and copper in e-cigarette aerosols Environmental Pollution 198:100–107 doi:10.1016/j.envpol.2014.12.033 [PubMed: 25577651]

Li L, Lin Y, Xia T, Zhu Y (2020) Effects of Electronic Cigarettes on Indoor Air Quality and Health Annual Review of Public Health 41:363–380 doi:10.1146/annurev-publhealth-040119-094043

Li N, Xia T, Nel AE (2008) The role of oxidative stress in ambient particulate matter-induced lung diseases and its implications in the toxicity of engineered nanoparticles Free Radical Biology and Medicine 44:1689–1699 doi:10.1016/j.freeradbiomed.2008.01.028 [PubMed: 18313407]

Mates JM (2000) Effects of antioxidant enzymes in the molecular control of reactive oxygen species toxicology Toxicology 153:83–104 doi:10.1016/s0300-483x(00)00306-1 [PubMed: 11090949]

McAuley TR, Hopke PK, Zhao J, Babaian S (2012) Comparison of the effects of e-cigarette vapor and cigarette smoke on indoor air quality Inhal Toxicol 24:850–857 doi:10.3109/08958378.2012.724728

Misra C, Singh M, Shen S, Sioutas C, Hall PA (2002) Development and evaluation of a personal cascade impactor sampler (PCIS) Journal of Aerosol Science 33:1027–1047 doi:10.1016/s0021-8502(02)00055-1

Nel A, Xia T, Meng H, Wang X, Lin S, Ji Z, Zhang H (2013) Nanomaterial toxicity testing in the 21st century: use of a predictive toxicological approach and high-throughput screening Accounts of chemical research 46:607–621 doi:10.1021/ar300022h [PubMed: 22676423]

Nemery B (1990) Metal toxicity and the respiratory tract European Respiratory Journal 3:202–219

O'Brien PJ, Siraki AG, Shangari N (2005) Aldehyde Sources, Metabolism, Molecular Toxicity Mechanisms, and Possible Effects on Human Health Critical Reviews in Toxicology 35:609–662 doi:10.1080/10408440591002183 [PubMed: 16417045]

Reuter S, Gupta SC, Chaturvedi MM, Aggarwal BB (2010) Oxidative stress, inflammation, and cancer How are they linked? Free Radical Biology and Medicine 49:1603–1616 doi:10.1016/j.freeradbiomed.2010.09.006 [PubMed: 20840865]

Romagna G, Allifranchini E, Bocchietto E, Todeschi S, Esposito M, Farsalinos KE (2013) Cytotoxicity evaluation of electronic cigarette vapor extract on cultured mammalian fibroblasts (ClearStream-LIFE): comparison with tobacco cigarette smoke extract Inhal Toxicol 25:354–361 doi:10.3109/08958378.2013.793439

Saffari A et al. (2014) Particulate metals and organic compounds from electronic and tobacco-containing cigarettes: comparison of emission rates and secondhand exposure Environ Sci-Process Impacts 16:2259–2267 doi:10.1039/c4em00415a [PubMed: 25180481]

Strongin RM (2019) E-Cigarette Chemistry and Analytical Detection In: Bohn PW, Pemberton JE (eds) Annual Review of Analytical Chemistry, Vol 12, vol 12. Annual Review of Analytical Chemistry pp 23–39. doi:10.1146/annurev-anchem-061318-115329

Ulloa L (2005) The vagus nerve and the nicotinic anti-inflammatory pathway Nature Reviews Drug Discovery 4:673 doi:10.1038/nrd1797 [PubMed: 16056392]

Valko M, Rhodes CJ, Moncol J, Izakovic M, Mazur M (2006) Free radicals, metals and antioxidants in oxidative stress-induced cancer Chemico-Biological Interactions 160:1–40 doi:10.1016/j.cbi.2005.12.009 [PubMed: 16430879]

Wang H et al. (2003) Nicotinic acetylcholine receptor α7 subunit is an essential regulator of inflammation Nature 421:384 doi:10.1038/nature01339 [PubMed: 12508119]

Xia T, Kovochich M, Nel A (2006) The role of reactive oxygen species and oxidative stress in mediating particulate matter injury Clin Occup Environ Med 5:817–836 doi:10.1016/j.coem.2006.07.005 [PubMed: 17110294]

Xia T et al. (2011) Decreased Dissolution of ZnO by Iron Doping Yields Nanoparticles with Reduced Toxicity in the Rodent Lung and Zebrafish Embryos ACS Nano 5:1223–1235 doi:10.1021/nn1028482 [PubMed: 21250651]

Zhao T, Shu S, Guo Q, Zhu Y (2016) Effects of design parameters and puff topography on heating coil temperature and mainstream aerosols in electronic cigarettes Atmospheric Environment 134:61–69 doi:10.1016/j.atmosenv.2016.03.027

Zhong ZY et al. (2016) NF-kappa B Restricts Inflammasome Activation via Elimination of Damaged Mitochondria Cell 164:896–910 doi:10.1016/j.cell.2015.12.057 [PubMed: 26919428]

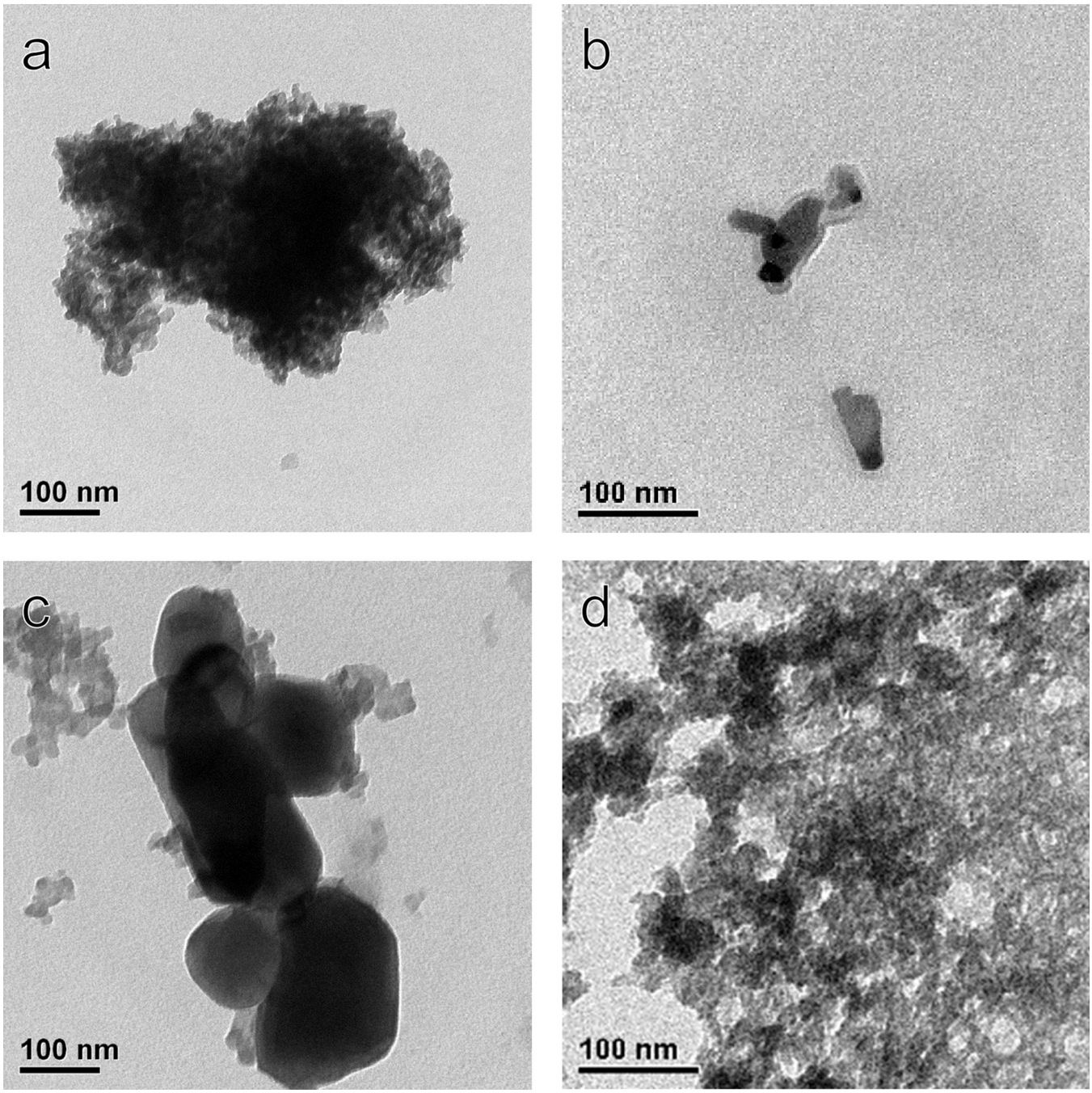

Figure 1.

Representative Transmission Electron Microscope (TEM) images to show the morphology of e-cigarette aerosol particles at 120 puffs with 0% nicotine (a), 120 puffs with 2.4% nicotine (b), 480 puffs with 0% nicotine (c), and 480 puffs with 2.4% nicotine (d).

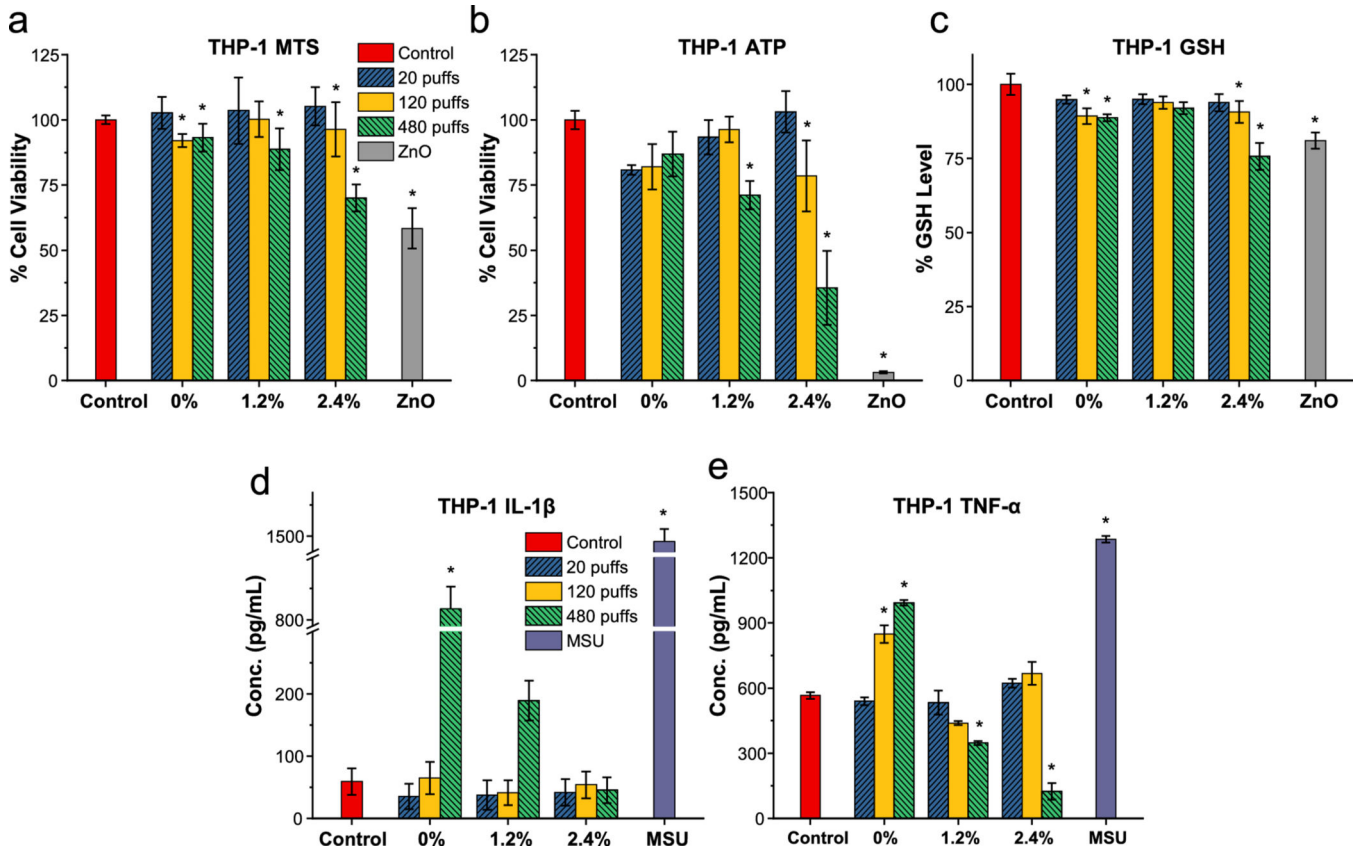

Figure 2.

(a,b) Determination of THP-1 cell proliferation by MTS and ATP assays after e-cigarette samples treatment for 24 h. The e-liquid with 0%, 1.2%, 2.4% nicotine concentration was collected for 20, 120, and 480 puffs to prepare the sample. ZnO NPs were used as a positive control with a concentration of 10 μg/mL. The cell culture medium was used as a negative control. The proliferation rate of the e-cigarette samples treated cells was normalized to the value of non-treated control cells, which was regarded as 100%. (c) Cellular GSH depletion in THP-1 cells. THP-1 cells were exposed to e-cigarette aerosol samples for 6 h. GSH levels were expressed as a percentage of the luminescence intensity compared to control cells. a, b, and c use the same legend. (d,e) IL-1β and TNF-α production in the supernatants obtained from Figure 2a. IL-1β and TNF-α levels were determined by ELISA. Monosodium urate (MSU) was used as a positive control with a concentration of 100 μg/mL. *$p < 0.05$, compared to control.

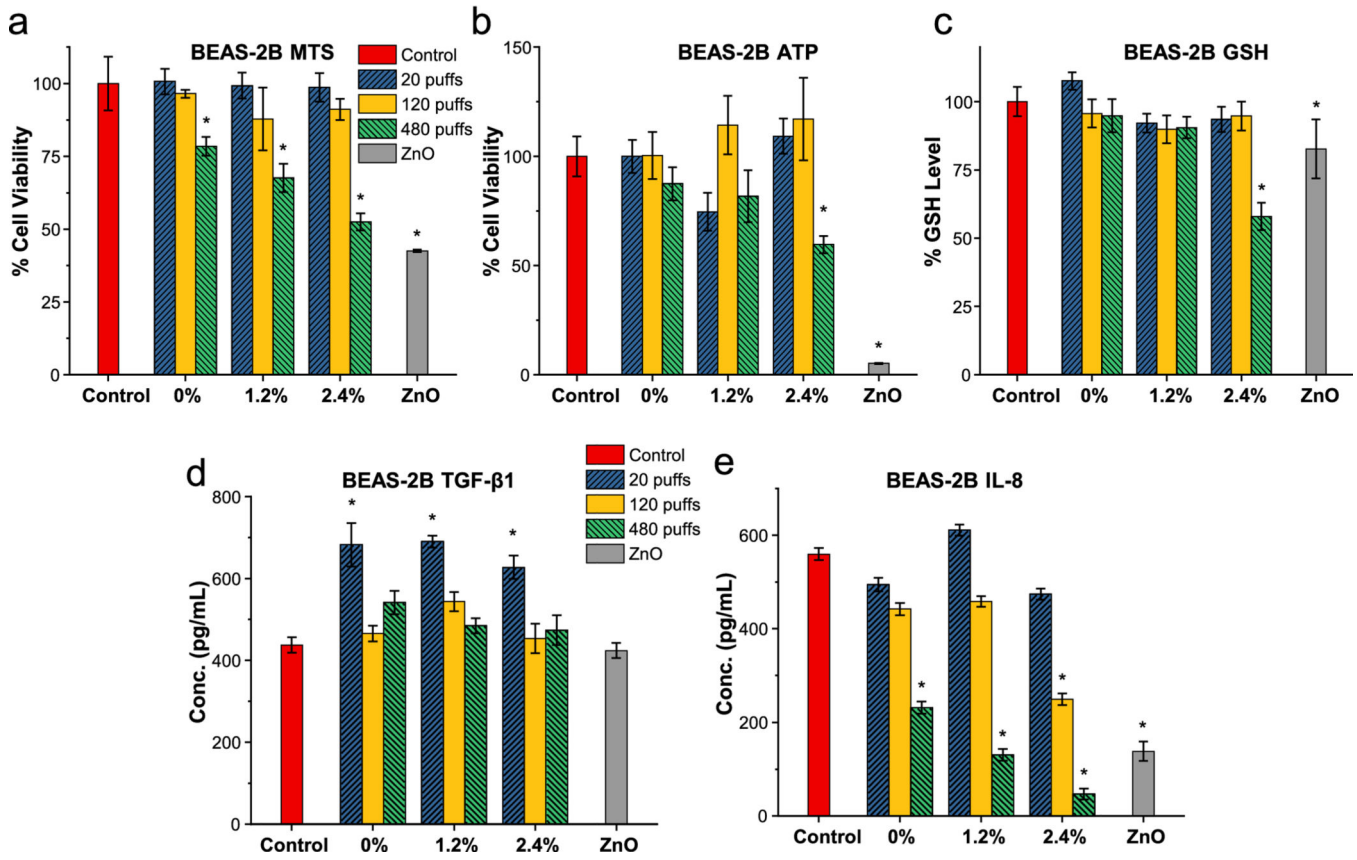

Figure 3.

(a,b) Determination of BEAS-2B cells proliferation by MTS and ATP assays after e-cigarette samples treatment for 24 h. The e-liquid with 0%, 1.2%, 2.4% nicotine concentration was collected for 20, 120, and 480 puffs to prepare the sample. ZnO NPs were used as a positive control with a concentration of 10 μg/mL. The cell culture medium was used as a negative control. The proliferation rate of the e-cigarette samples treated cells was normalized to the value of non-treated control cells, which was regarded as 100%. (c) Cellular GSH depletion in BEAS-2B cells. BEAS-2B cells were exposed to e-cigarette aerosol samples for 6 h. GSH levels were expressed as a percentage of the luminescence intensity compared to control cells. a, b, and c use the same legend. (d,e) TGF-β1 and IL-8 production in the supernatants obtained from Figure 3a. TGF-β1 and IL-8 levels were determined by ELISA. ZnO NPs were used as the positive control with a concentration of 10 μg/mL. *$p < 0.05$, compared to control.

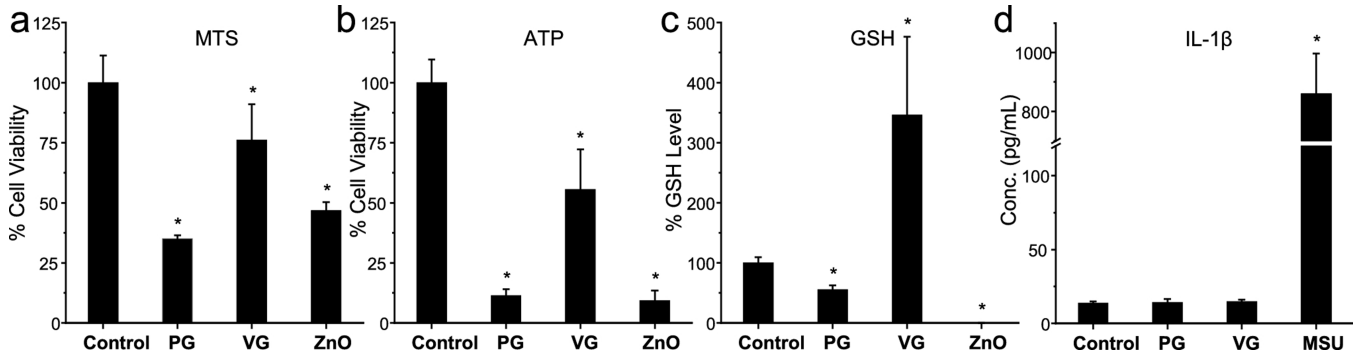

Figure 4.

Cellular viability and oxidative stress in THP-1 cells exposed to PG, VG aerosol samples, and samples with different nicotine. The number of puffs is 120. (a) Use of a MTS assay in THP-1 cells, exposure to pure PG and pure VG aerosol samples for 24 h. The culture medium was used as control and ZnO NPs (10 μg/mL) was the positive control. (b) Use of an ATP assay to assess the cell viability of THP-1 cells, using the same protocol as in MTS assay. (c) Cellular GSH depletion in THP-1 cells was conducted by using luminescence-based GSH-Glo assay. THP-1 cells were exposed to e-cigarette aerosol samples for 6 h. GSH levels were expressed as a percentage of the luminescence intensity compared to control cells. $*p < 0.05$, compared to control. (d) IL-1β production in the supernatants obtained from Figure 5a. IL-1β levels were determined by ELISA. $*p < 0.05$ compared to control.

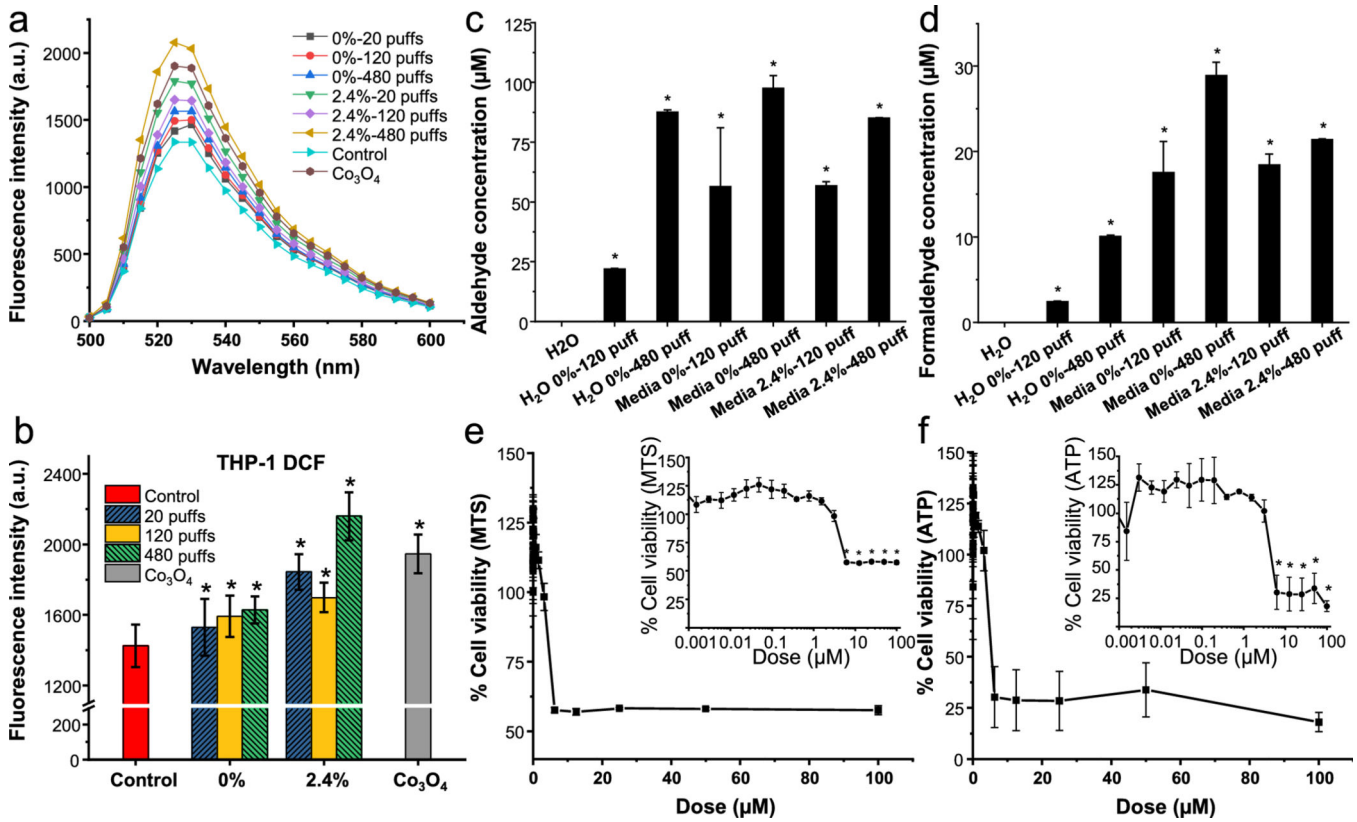

Figure 5.

DCF fluorescence: (a) 29 μmol/L of DCF was incubated with e-cigarette samples for 3 h. Fluorescence emission spectra were collected at 500–600 nm with excitation at 490 nm. Co_3O_4 NPs (10 μg/mL) was the positive control. (b) The intensity of DCF fluorescence at 525 nm. *$p < 0.05$, compared to H_2O. Quantification of aldehyde and formaldehyde content. (c) The aldehyde level in the e-cigarette aerosol samples was determined using a colorimetric aldehyde assay kit. After incubation with the aldehyde detection reagent for 1 h, the supernatants were used for assessment of absorbance at 405 nm in a SpectroMax M5e microplate reader. (d) The formaldehyde level in the e-cigarette aerosol samples was determined using a fluorometric aldehyde assay kit. After incubation with the detection reagent for 0.5 h, the fluorescence was detected at Ex/Em = 535/587 nm with a SpectroMax M5e microplate reader. Use of the MTS assay (e) and ATP assay (f) to determine the cellular viability of THP-1 cells exposed to formaldehyde. The inset shows the detail by using Logarithmic scale. All the MTS and ATP values were normalized vs. non-treated controls representing 100% cell viability. *$p < 0.05$ compared to control.

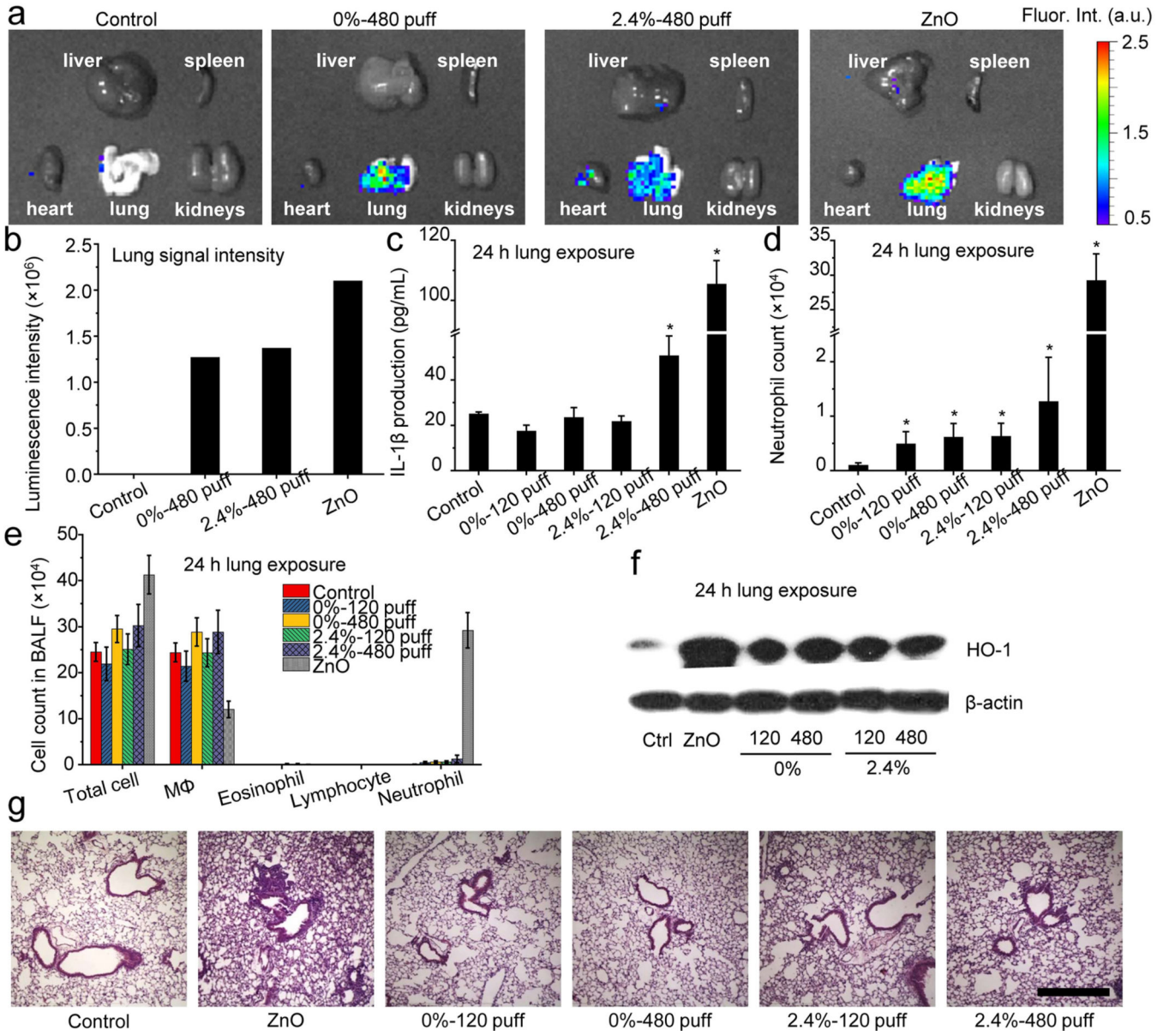

Figure 6.

Acute pulmonary inflammatory effect in mice. (a) Transgenic mice were exposed to ZnO and e-cigarette aerosols with different nicotine levels at two different doses for 24 h and imaged by IVIS. (b) The luminescence intensity of the lung area. Wild-type animals were euthanized at 24 h post-exposure, and BALF was collected to determine (c) IL-1β production, (d) neutrophil, and (e) differential cell count. *$p < 0.05$. (f) The lung tissues were collected to assess HO-1 expression by western blotting (ZnO NPs at 2 mg/kg was used as positive controls). (g) The lung tissue from the same animals was stained by H&E method. The scale bar corresponds to 500 μm.

Table 1.

Hydrodynamic size (nm) and zeta potential (mV) of e-cigarette samples in water.

Sample in water	Hydrodynamic Size (nm)	Zeta potential (mV)
0%−20 puffs	454 ± 161	−19.8 ± 0.5
0%−120 puffs	281 ± 59	−9.4 ± 1.0
0%−480 puffs	219 ± 79	−9.3 ± 0.3
2.4%−20 puffs	129 ± 59	−20.5 ± 1.2
2.4%−120 puffs	160 ± 40	−39.8 ± 2.2
2.4%−480 puffs	259 ± 51	−27.2 ± 2.3

Table 2.

Element analysis using inductively coupled plasma mass spectrometer (ICP-OES) in e-cigarette samples. (average ± stdev, ng/mL, ppb)

element	0%−20 puffs	0%−120 puffs	0%−480 puffs	2.4%−20 puffs	2.4%−120 puffs	2.4%−480 puffs
B	8.12±0.04	11.94±0.04	35.54±0.06	7.82±0.27	14.00±0.49	24.97±0.29
Na	677.39±2.85	866.63±0.47	1463.23±8.4	606.55±6.8	980.53±3.23	1422.84±11.79
Mg	168.64±0.91	213.21±1.71	545.46±3.85	147.72±0.48	201.43±0.35	196.12±2.01
Si	169.10±1.66	223.34±2.33	1074.02±22.95	155.03±2.03	234.00±1.88	201.51±2.91
P	558.18±25.25	979.19±25.5	3742.15±84.75	390.24±9.35	376.96±8.50	477.09±4.88
S	314.17±26.02	345.83±11.81	264.17±9.46	242.92±7.91	369.78±25.62	932.44±36.30
K	109.40±1.72	116.98±0.53	214.82±2.85	84.83±2.55	133.95±1.74	204.81±2.72
Ca	952.03±16.37	1553.32±3.7	3845.73±31.75	651.77±9.97	791.71±3.467	838.86±4.75
Fe	0.00	0.00	0.00	0.00	115.29±0.6	137.21±1.51
Cu	n/a	n/a	7.17±0.05	n/a	5.58±0.15	19.82±0.13
Zn	19.57±0.54	21.98±0.09	12.02±0.21	19.80±0.16	9.67±0.288	16.87±0.17
Sr	5.65±0.04	8.39±0.12	15.31±0.17	4.04±0.06	6.00±0.058	5.87±0.01
Nb	1.59±0.09	6.95±0.45	6.16±0.77	0.08±0.02	0.19±0.01	0.42±0.02
Sn	25.26±0.38	30.28±0.15	45.75±2.72	22.55±1.00	27.98±0.72	30.35±2.15
I	3.27±0.26	3.15±0.15	2.42±0.26	0.00	0.00	0.00
Ta	0.92±0.01	4.80±0.17	11.43±0.99	0.22±0.03	0.46±0.00	0.75±0.03
W	1.08±7.15	1.45±8.96	2.04±11.67	0.83±6.65	1.03±2.32	1.06±11.28
Pb	0.66±0.00	0.47±0.01	0.43±0.01	1.42±0.03	0.51±0.01	0.58±0.01